Analyst

COMMUNICATION

View Article Online
View Journal

Cite this: DOI: 10.1039/c6an00675b

Received 22nd March 2016,
Accepted 26th April 2016

DOI: 10.1039/c6an00675b

www.rsc.org/analyst

Electrochromic sensing platform based on steric hindrance effects for CEA detection†

Qingfeng Zhai,[a,b] Xiaowei Zhang,[a,b] Yong Xia,[a] Jing Li*[a] and Erkang Wang*[a]

In this work, an electrochromic sensing platform with prussian blue (PB) as the indicator was proposed for signaling carcinoembryonic antigen (CEA) using the bipolar electrode (BPE) system. The CEA aptamer was pre-anchored on the anode pole of the BPE for capturing CEA through strong binding affinity. The presence of CEA induced the increase of steric hindrance and led to lower electrochemical currents. Due to the quantitative relationship between the two reactions occurring at both ends of the BPE, the amount of deposited PB *in situ* can be used as an indicator for reporting target protein concentration. Using CEA concentration in normal human serum as a reference (5 ng mL^{-1}), this electrochromic sensing platform can be used for distinguishing persons with cancer from normal humans easily and quickly, which is very important for subsequent treatment of patients. This novel electrochromic platform has great selectivity for target tumor proteins and provides a fast, visual method for CEA detection. Finally, the proposed biosensor can be applied to detect CEA in human serum, which holds great potential for point-of-care diagnostics combined with the advantage of the closed BPE system.

Introduction

According to the U.S. National Cancer Institute, cancer has become the number two leading cause of death.[1,2] As a consequence, early accurate cancer identification and detection are crucial for patient survival and successful prognosis of cancers.[3] Carcinoembryonic antigen (CEA), an acidic glycoprotein with a molecular weight of about 180 kDa, is known to be one of the most important tumor markers.[4] Various carcinomas are related to CEA,[5,6] such as lung, breast and rectal cancer. Thus far, fluorometric analysis,[7,8] radioimmunoassay,[9] enzyme-linked immunosorbent assay,[10,11] chemiluminescence immunoassay[12,13] and other methods[14,15] have been developed for CEA detection. Among these methods, electrochemical methods have attracted considerable interest due to advantages of high sensitivity, low cost and portability.[16–18] In most cases, electrochemical sensors for CEA were based on labeled[19] or solid-state electrochemical probes as reporters,[20] which require a complex modification process. In addition, little attention was paid to high-throughput assays among current electrochemical sensors since the signal readout often requires the involvement of expensive electrochemical workstations to complete. Developing label-free and high-throughput approaches to distinguish patients with cancer from those without is very important for point-of-care diagnostics.[21–23] Steric hindrance effects provided an effective tool for label-free electrochemical determination of target.[24–26] When the target molecule is bound to the surface of the electrode, the electron transfer of the redox molecule can be inhabited, and current decreased.[27,28] Based on this steric hindrance mechanism, Ban and co-workers[29] developed an electrochemical aptasensor for cardiac troponin I detection in the presence of a ferrocene-modified silica nanoparticle redox probe.

The bipolar electrode (BPE) has recently attracted considerable attention in bioanalysis[30–32] and has been widely used for detection of prostate-specific antigen (PSA),[33] DNA,[34,35] cancer biomarkers,[36,37] and so on. It can act as both anode and cathode without any direct electrical connection under an even electrical field over the solution, which offers good opportunities to control large-scale BPEs in parallel for high-throughput analysis. To date, the signal readout for this detection was mostly focused on electrochemiluminescence,[38,39] which was often achieved *via* expensive instruments for collecting the output signal. In order to achieve visual target detection, Crooks and co-workers[40] reported an electrochemical sensing platform using a prussian blue (PB) spot that electrodeposited on an ITO film as the electrochromic indicator for visual detection of glucose and H_2O_2. Based on this electrochromic principle, our group[41,42] developed a renewable display platform for screening the activity of catalysts with the naked eye.

[a]State Key Laboratory of Electroanalytical Chemistry, Changchun Institute of Applied Chemistry, Chinese Academy of Sciences, Changchun, Jilin 130022, China. E-mail: lijingce@ciac.ac.cn, erkwang@ciac.ac.cn; Fax: +86-431-85689711; Tel: +86-431-85262003

[b]University of Chinese Academy of Sciences, Beijing, 100039, China

†Electronic supplementary information (ESI) available: Experimental details. See DOI: 10.1039/c6an00675b

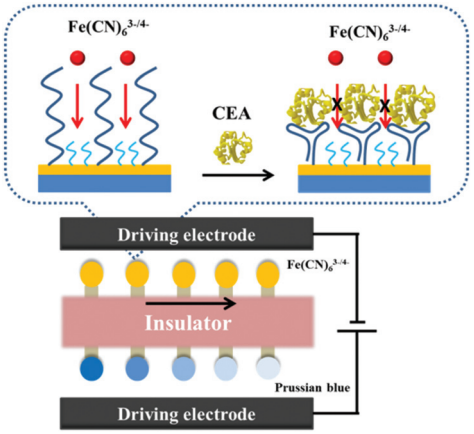

Scheme 1 Schematic illustration of closed bipolar electrochromic strategy for high-throughput analysis of CEA.

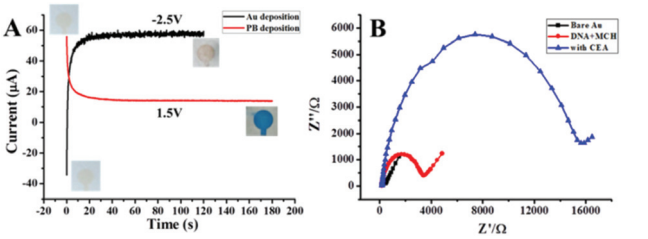

Fig. 1 (A) Current change of closed BPE array under certain voltage for Au and PB deposition, respectively. (B) EIS of the CEA aptamer-modified Au electrode before and after incubation with 5 ng per mL CEA in 0.1 M NaCl + 5 mM $[Fe(CN)_6]^{3-/4-}$ solution.

Inspired by the unique steric hindrance mechanism and BPE, a novel, high-throughput and visual sensing platform for CEA detection with the closed BPE arrays was demonstrated. First, the single-strand DNA aptamer of CEA was attached on BPE anodes to capture CEA due to strong and specific binding affinity. When CEA were bound on the electrode surface, the electron transfer of redox molecule probe ($[Fe(CN)_6]^{3-/4-}$) was inhibited due to steric hindrance. On the basis of the quantitative relation between the two reactions occurring at both ends of the BPE, the current passing the closed BPE cathode was accordingly decreased, which influenced the amount of PB deposited at the BPE cathode pole and can be recognized by the naked eye. The electrochromic detection system offers great sensitivity for target molecules and provides fast and visual detection of CEA concentration. Meanwhile, the proposed biosensor can be applied to detect CEA in human serum, which holds the potential in the field of point-of-care diagnostics combined with advantages of the closed BPE system (see Scheme 1).

Results and discussion

The standard photolithographic technique was used to fabricate the ITO electrode array, and the closed bipolar system was achieved by bonding a PDMS membrane with two reservoirs on the ITO substrate. Au film was deposited on the electrode surface, as shown in Scheme 1. CEA aptamer DNA was modified on the Au film *via* formation of the sulfur–gold bond and then backfilled in non-specific binding sites with MCH. When CEA is introduced into the sensing channel, the target CEA can bind with the recognition element on the electrode surface through specific affinity and induced the aptamer DNA structural change.[8] CEA is a biological protein molecule of about 180 kDa; it may be bound on the electrode surface to effectively retard the interfacial electron-transfer kinetics of the redox probes in the sensing channel due to the protein's steric hindrance effects. Due to the related quantitation between the two BPE poles, the current through the BPE cathodes was also decreased and thus influenced the amount of PB. The amount of deposited PB was dependent on CEA concentration, which provides the basis for CEA detection.

Au film was selected and deposited onto the BPE anode through electrochemical deposition using driving 2.5 V for 120 s. As shown in Fig. 1A, the current has an obvious change in the first 20 s and then maintains a stable value. As seen in the photograph, the color of the electrode was changed to yellow, which indicated that Au was successfully deposited on the electrode surface. To verify the *in situ* deposition of the electrochromic material, driving voltage of 1.5 V was used for BP deposition at the BPE cathodes. Like the Au film deposition, an obvious current change at the initial stage was observed due to BP deposition, and subsequently the current maintained a stable value (Fig. 1B) accompanying the color change to blue. The amount of deposited PB can be adjusted by controlling deposition time. Consequently, it can be used as the indicator for reporting the target concentration.

In order to verify the change in electron-transfer resistance induced by the CEA, electrochemical impedance spectra (EIS) were collected with a gold electrode using $[Fe(CN)_6]^{3-/4-}$ as the indicator. The Nyquist plots are displayed in Fig. 1B; a very small semicircle domain was obtained with the bare Au electrode, indicating low electron-transfer resistance (Ret). After incubation with CEA aptamer DNA and MCH, impedance obviously increased (Ret = 3.5×10^3 Ω) due to the electrostatic repulsive force between the negative charged interface and $[Fe(CN)_6]^{3-/4-}$ anions. The sensing interface was then used for capturing CEA and the impedance spectrum recorded. The Ret was significantly increased from 3.5×10^3 Ω to 1.6×10^4 Ω, illustrating the decreased efficiency in electron transfer resulting from steric hindrance after protein binding.

The fabricated sensing interface was used for response to different concentrations of CEA for high-throughput assays using closed BPE arrays. Different concentrations of CEA were introduced into the sensing channels and incubated for 1 h. 5 mM $[Fe(CN)_6]^{3-/4-}$ and PB deposition solution (2.5 mM $FeCl_3$ + 2.5 mM $K_3[Fe(CN)]_6$ + 0.1 M HCl + 0.1 M KCl)) were injected into the sensing array channel and reporting channel, respectively. Then a driving voltage of 1.5 V was applied on the driving electrodes for 180 s, and PB was deposited on the electrode of BPE arrays. Results are shown in Fig. 2A. As displayed,

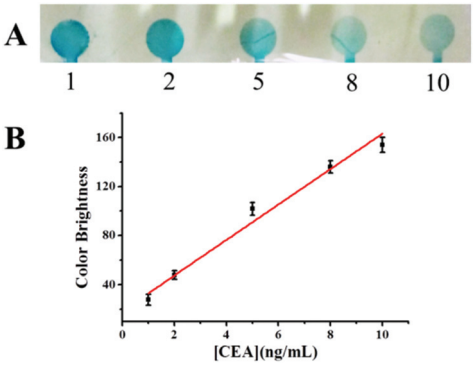

Fig. 2 Closed bipolar electrochromic strategy for detecting different concentrations of CEA from 1 to 10 ng mL^{-1}. (A) Photographs of PB spots in different concentrations of CEA. (B) Linear relationship between CEA concentration and color brightness of PB spots.

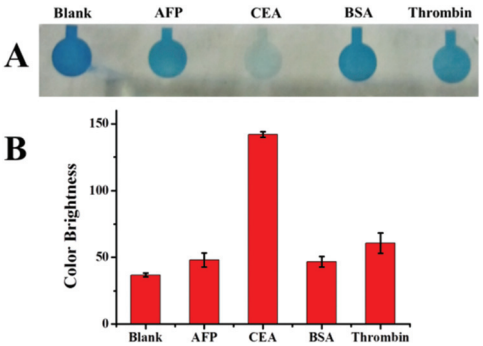

Fig. 3 Closed bipolar electrochromic strategy for detecting different concentrations of CEA from 1 to 10 ng mL^{-1}. (A) Photographs of PB spots in different concentrations of CEA. (B) Linear relationship between CEA concentration and color brightness of PB spots.

the amount of deposited PB was decreased with the increase in CEA concentrations from 1 ng mL^{-1} to 10 ng mL^{-1}. Correspondingly, the color of the PB spot changed from blue to nearly colorless. To further confirm results, the Nyquist plots for different concentrations of CEA were recorded as shown in Fig. S3A.† The Ret increased from 3450 to 28 700 and increased Ret signals were directly related to CEA concentration from 1 ng mL^{-1} to 10 ng mL^{-1}, illustrating the steric hindrance effect on electron transfer.

CEA concentration in normal human serum is about 5 ng mL^{-1}.[5] Thus, using this value as a reference, higher or lower CEA concentration can be observed directly by the naked eye. Experimental results confirmed that the designed electrochromic strategy could be used for confirming people with cancer risk with the naked eye. In order to analyze CEA concentration quantitatively, chip reader software was installed on an intelligent phone[43,44] for analyzing the color brightness of PB spots; results are shown in Fig. 2B. We found that PB spot brightness was increased according to CEA concentration, which has a strong linear relationship in the range of 1 to 10 ng mL^{-1}.

CEA is a typical tumor biomarker and we hope that our designed electrochromic sensor can be used for clinical diagnosis.[45] Such sensor must possess high specificity for target molecules compared with other interfering substances. In order to explore selectivity and specificity of our electrochromic strategy, control experiments were performed. Three typical proteins—AFP, BSA and thrombin—were chosen as control molecules. According to the photographic results in Fig. 3A, the presence of low CEA concentration (10 ng mL^{-1}) causes a remarkable color change (blue to light-blue) due to formation of a CEA-aptamer complex. While in the presence of even 5-fold excess of interferential proteins (50 ng mL^{-1}) under the same condition, a very small color change was observed compared with the blank experiment. The signal readout can also be recognized from the color brightness histogram of PB spots in different protein samples (Fig. 3B). Results showed that selectivity of the electrochromic strategy toward CEA was very good with recognized CEA aptamer and not greatly affected by other interfering proteins, which can be used for target CEA selectively detected by the naked eye.

Table 1 CEA concentration in human serum detected by our device

Sample	Photographs	Results from our device	Data from hospital	Comparative deviation
Human serum		5.41	5.64	4.08%
		3.67	3.56	3.09%
		9.78	9.38	4.26%

Direct determination of CEA level in human serum is very important for early cancer diagnosis. The practical application of the electrochromic sensor based on closed BPE arrays was demonstrated in real human serum (obtained from First Hospital of Jilin University, Changchun). Results are given in Table 1. Using the CEA concentration in normal human serum as a reference point (≈5 ng mL^{-1}),[6] and higher or lower levels can be observed directly by the naked eye through the designed electrochromic strategy. CEA contents of real human serum samples identified by our strategy were in good agreement with results provided by the hospital, which indicated that the electrochromic platform has great promise for CEA detection in real samples.

Conclusions

In summary, an electrochromic sensing platform for CEA detection was presented based on steric hindrance effects. The aptamer modified on the anode pole of the BPE can bind CEA protein through the strong affinity. CEA as a protein has a molecular weight of about 200 kDa, which can effectively retard the interfacial electron-transfer kinetics of the redox probes. Thus the electron transfer resistance (Ret) of the platform was increased and the current passed through the closed BPE was decreased, which made the amount of PB deposited in the cathode of BPE decrease. Meanwhile, the deposited amount was dependent on CEA concentration and it can be observed

with the naked eye. The concentration of CEA in normal human serum is less than about 5 ng mL^{-1}; this electrochromic sensing platform can be used for distinguishing the person with cancer from a normal human with the naked eye simply and quickly. It not only saves time and lowers costs, but also is very important for high-throughput assays of CEA detection. CEA protein was successfully detected in human serum solution with satisfactory performance levels. This novel electrochromic platform has great sensitivity for target tumor proteins and provides a fast and visual method for CEA detection. Combined with the unique feature of the BPE to control large-scale arrays and label-free strategy, the proposed biosensor may be used as a novel platform for CEA detection in point-of-care diagnostics.

Acknowledgements

This work was supported by the National Natural Science Foundation of China (grants 21190040 and 21427811) and Youth Innovation Promotion Association CAS (2016208).

Notes and references

1 W. Zhou, J. Su, Y. Chai, R. Yuan and Y. Xiang, *Biosens. Bioelectron.*, 2014, **53**, 494–498.
2 S. T. Sanjay, G. Fu, M. Dou, F. Xu, R. Liu, H. Qi and X. Li, *Analyst*, 2015, **140**, 7062–7081.
3 D. A. Giljohann and C. A. Mirkin, *Nature*, 2009, **462**, 461–464.
4 S. Viswanathan, C. Rani, A. Vijay Anand and J. A. Ho, *Biosens. Bioelectron.*, 2009, **24**, 1984–1989.
5 D. Faraggi and A. Kramar, *Urol. Oncol.-Semin. Ori.*, 2000, 211–213.
6 M. Duffy, A. van Dalen, C. Haglund, L. Hansson, R. Klapdor, R. Lamerz, O. Nilsson, C. Sturgeon and O. Topolcan, *Eur. J. Cancer*, 2003, **39**, 718–727.
7 M. He and Z. Liu, *Anal. Chem.*, 2013, **85**, 11691–11694.
8 Z. Lin, G. Zhang, W. Yang, B. Qiu and G. Chen, *Chem. Commun.*, 2012, **48**, 9918–9920.
9 D. Thomson, J. Krupey, S. Freedman and P. Gold, *Proc. Natl. Acad. Sci. U. S. A.*, 1969, **64**, 161–167.
10 A. Bhimji, A. A. Zaragoza, L. S. Live and S. O. Kelley, *Anal. Chem.*, 2013, **85**, 6813–6819.
11 Y. Cai, H. Li, Y. Li, Y. Zhao, H. Ma, B. Zhu, C. Xu, Q. Wei, D. Wu and B. Du, *Biosens. Bioelectron.*, 2012, **36**, 6–11.
12 J. Lin and H. Ju, *Biosens. Bioelectron.*, 2005, **20**, 1461–1470.
13 J. Yakovleva, R. Davidsson, A. Lobanova, M. Bengtsson, S. Eremin, T. Laurell and J. Emnéus, *Anal. Chem.*, 2002, **74**, 2994–3004.
14 J. Liu, J. Wang, T. Wang, D. Li, F. Xi, J. Wang and E. Wang, *Biosens. Bioelectron.*, 2015, **65**, 281–286.
15 L. Ge, W. Wang, T. Hou and F. Li, *Biosens. Bioelectron.*, 2016, **77**, 220–226.
16 M. S. Wilson, *Anal. Chem.*, 2005, **77**, 1496–1502.
17 S. Xu, Y. Liu, T. Wang and J. Li, *Anal. Chem.*, 2011, **83**, 3817–3823.
18 J. Gao, Z. Guo, F. Su, L. Gao, X. Pang, W. Cao, B. Du and Q. Wei, *Biosens. Bioelectron.*, 2015, **63**, 465–471.
19 B. V. Chikkaveeraiah, A. A. Bhirde, N. Y. Morgan, H. S. Eden and X. Chen, *ACS Nano*, 2012, **6**, 6546–6561.
20 J. Han, J. Ma and Z. Ma, *Biosens. Bioelectron.*, 2013, **47**, 243–247.
21 G. Zheng, F. Patolsky, Y. Cui, W. U. Wang and C. M. Lieber, *Nat. Biotechnol.*, 2005, **23**, 1294–1301.
22 H. Li, Q. Wei, J. He, T. Li, Y. Zhao, Y. Cai, B. Du, Z. Qian and M. Yang, *Biosens. Bioelectron.*, 2011, **26**, 3590–3595.
23 H. Shu, W. Wen, H. Xiong, X. Zhang and S. Wang, *Electrochem. Commun.*, 2013, **37**, 15–19.
24 T. Yang, Q. Li, X. Li, X. Wang, M. Du and K. Jiao, *Biosens. Bioelectron.*, 2013, **42**, 415–418.
25 B. Chen, Y. Ding, X. Li, W. Zhu, J. P. Hill, K. Ariga and Y. Xie, *Chem. Commun.*, 2013, **49**, 10136–10138.
26 T. Wei, Y. Chen, W. Tu, Y. Lan and Z. Dai, *Chem. Commun.*, 2014, **50**, 9357–9360.
27 S. S. Mahshid, S. Camiré, F. Ricci and A. Vallée-Bélisle, *J. Am. Chem. Soc.*, 2015, **137**, 15596–15599.
28 S. H. Hyun, D. K. Park, A. Kang, S. Kim, D. Kim, Y. M. Shin, J.-J. Song and W. S. Yun, *Appl. Phys. Lett.*, 2016, **108**, 093101.
29 H. Jo, H. Gu, W. Jeon, H. Youn, J. Her, S. K. Kim, J. Lee, J. H. Shin and C. Ban, *Anal. Chem.*, 2015, **87**, 9869–9875.
30 X. Zhang, C. Chen, J. Li, L. Zhang and E. Wang, *Anal. Chem.*, 2013, **85**, 5335–5339.
31 S. E. Fosdick, K. N. Knust, K. Scida and R. M. Crooks, *Angew. Chem., Int. Ed.*, 2013, **52**, 10438–10456.
32 J. P. Guerrette, S. J. Percival and B. Zhang, *J. Am. Chem. Soc.*, 2013, **135**, 855–861.
33 M.-S. Wu, D.-J. Yuan, J.-J. Xu and H.-Y. Chen, *Chem. Sci.*, 2013, **4**, 1182.
34 M. S. Wu, G. S. Qian, J. J. Xu and H. Y. Chen, *Anal. Chem.*, 2012, **84**, 5407–5414.
35 J. D. Besant, J. Das, I. B. Burgess, W. Liu, E. H. Sargent and S. O. Kelley, *Nat. Commun.*, 2015, **6**, 6978.
36 Q. Zhai, X. Zhang, Y. Han, J. Zhai, J. Li and E. Wang, *Anal. Chem.*, 2016, **88**, 945–951.
37 M. S. Wu, Z. Liu, H. W. Shi, H. Y. Chen and J. J. Xu, *Anal. Chem.*, 2015, **87**, 530–537.
38 W. Zhan, J. Alvarez and R. M. Crooks, *J. Am. Chem. Soc.*, 2002, **124**, 13265–13270.
39 K.-F. Chow, F. Mavré, J. A. Crooks, B.-Y. Chang and R. M. Crooks, *J. Am. Chem. Soc.*, 2009, **131**, 8364–8365.
40 H. Liu and R. M. Crooks, *Anal. Chem.*, 2012, **84**, 2528–2532.
41 X. Zhang, C. Shang, W. Gu, Y. Xia, J. Li and E. Wang, *ChemElectroChem*, 2016, **3**, 383–386.
42 X. Zhang, L. Zhang, Q. Zhai, W. Gu, J. Li and E. Wang, *Anal. Chem.*, 2016, **88**, 2543–2547.
43 P. B. Lillehoj, M.-C. Huang, N. Truong and C.-M. Ho, *Lab Chip*, 2013, **13**, 2950–2955.
44 J. X. Wong, F. S. Liu and H.-Z. Yu, *Anal. Chem.*, 2014, **86**, 11966–11971.
45 Z.-M. Zhou, J. Zhou, J. Chen, R.-N. Yu, M.-Z. Zhang, J.-T. Song and Y.-D. Zhao, *Biosens. Bioelectron.*, 2014, **59**, 397–403.

